

Molecular dynamics with phase-shift-based electronic stopping for calibration of ion implantation profiles in crystalline silicon

H.Y. Chan ^{a,e,*}, K. Nordlund ^b, H.-J.L. Gossmann ^c, M. Harris ^c, N.J. Montgomery ^d,
C.P.A. Mulcahy ^d, S. Biswas ^d, M.P. Srinivasan ^a, F. Benistant ^e, C.M. Ng ^e, Lap Chan ^e

^a Department of Chemical and Biomolecular Engineering, National University of Singapore, 10 Kent Ridge Crescent, Singapore 119260, Singapore

^b Accelerator Laboratory, P.O. Box 43, FIN-00014 University of Helsinki, Finland

^c Axcelis Technologies, 108 Cherry Hill Drive, Beverly, MA 01915-1053, USA

^d Cascade Scientific Ltd, ETC Building, Brunel Science Park, Uxbridge UB8 3PH, U.K.

^e Chartered Semiconductor Manufacturing Ltd., 60 Woodlands Industrial Park D, Street Two, Singapore 738406, Singapore

Available online 19 October 2005

Abstract

Prediction of the final dopant positions after ion implantation has always been strongly influenced by the choice of stopping models. A molecular dynamics (MD) method is used in this work; the nuclear stopping is treated by accurate pair potentials calculated by density functional theory (DFT). The slowing down due to collisions with electrons will be described by both a non-local semi-empirical model and a local model based on Fermi level phase shift factors. Comparisons with experimental data using both models show that a local pair-specific electronic stopping model is essential in accurately predicting range profiles for any element even at low implant energies where nuclear effects are dominant.

© 2005 Elsevier B.V. All rights reserved.

Keywords: Molecular dynamics; Interatomic potential; Nuclear stopping; Electronic stopping

1. Introduction

Atomistic simulations have been widely used in calculations of the distribution of dopants in target materials. Programs based on the Binary Collision Approximation (BCA) describe the motion of randomly generated energetic particles by sequences of binary collisions with target atoms in the closest environment of the particle trajectories [1–3]. They are also called Monte Carlo (MC) codes due to the use of random numbers. Another atomistic technique, Molecular Dynamics (MD), calculates the trajectories of a system of atoms by numerically solving Newton's equations of motion. The disparity in computational burden for both techniques has rendered BCA codes effective in predicting range profiles up to the million electronvolts range [4], useful for CMOS retrograde well implants and latch-up discharge protection. Sub-kilo-electronvolts implants however are becoming more crucial as

transistor technology traverses the nano-regime, particularly for source-drain contact and extension. MD has been touted to replace BCA in the low energy regime due to several factors. Collision cascades formed at low energies is small; MD is no longer limited by time and space. Moreover, BCA can be expected to fail as simultaneous multi-body collisions come into play at low energies. For this work, the ion range distributions will be calculated by MD where nuclear effects are treated with potentials calculated from first-principles. Electronic losses are treated with both a non-local semi-empirical electronic stopping model and a local model based on Fermi level phase shifts. Comparisons against experiments show excellent predictive capability of the local model over the non-local model for any elemental profile in crystalline silicon obtained at low and intermediate energies in any implant direction, even in channelling directions where the atom and electron densities are significantly lower than average.

2. Molecular dynamics simulations

All simulations shown in this work have been obtained with the MD code, MDRANGE [5]. The Recoil Ion Approximation

* Corresponding author. Blk 103, Bishan Street 12, #18-272, Singapore 570103, Singapore. Tel.: +65 97514678; fax: +65 62844215.

E-mail address: engp1438@nus.edu.sg (H.Y. Chan).

(RIA) has been employed, where only the ion-recoil interactions are considered. This is based on the assumption that the interactions between the ion and its nearest neighbors are much stronger than the lattice–lattice interactions. RIA has been shown to reduce the computational burden, with little effect on the final range profiles [5]. In all the simulations, initially crystalline silicon was used as a target material. The ambient temperature, 300 K was used and realistic atomic thermal displacements were obtained by setting the Debye temperature of silicon to 519 K [6]. The number of simulated ions used was 20,000, and deemed sufficient for good statistics. In order to determine the profiles over more than four decades of concentration, a version of Beardmore’s rare-event algorithm [7] was implemented. An atom splitting scheme is employed so that at certain splitting depths the ion is split into two virtual ions with a statistical weight of half that of the unsplit ion [8]. This ensures accurate dopant profiles with good statistics and feasible computational overhead. The effect of damage build-up on range profiles at high implant doses is especially pronounced and is taken into account by changing the material structure in front of the path of the incoming ion [9].

2.1. Nuclear effects: ZBL versus DMOL potential

The energy loss to target nuclei involves primarily the study of screened Coulomb collisions between two colliding atoms since the interaction at very small inter-atomic distances is essentially Coulombic. Amongst the many semi-empirical and theoretical repulsive potentials that have been proposed over the years, the “universal” repulsive potential given by Ziegler, Biersack and Littmark [1], the so-called ZBL potential constructed by fitting a universal screening function to theoretically obtained potentials calculated for 261 atom pairs has been most commonly used in BCA as well as MD codes. While the pair potential can well describe the projectile–nucleus interaction at high velocities, the validity of the solely repulsive ZBL potential becomes questionable at low velocities, since it cannot account for attractive forces that start to dominate as the incoming ion slows down in the host material.

Density functional theory (DFT) calculations utilizing numerical basis sets have been found to provide potentials which are significantly improved compared to the ZBL

potential [10]. Unlike the ZBL potential which is repulsive over the entire interatomic range, such potentials calculated from first-principles consist of a steep repulsive region and an attractive well. In this work, similar potential energy calculations for many dopant–silicon systems have been made. The DMOL [11] package was used, with hydrogenic orbitals included for all systems studied. These DFT calculated potentials will be denoted as DMOL potentials thereafter. The nuclear effect of both ZBL and DMOL potentials on the range profiles can be isolated by neglecting all electronic losses. Profiles obtained by Secondary Ion Mass Spectrometry (SIMS) were compared against MD simulations for two systems differing in mass, B–Si and As–Si. Figs. 1 and 2 show the effect of the interatomic potential on light and heavy element systems at both low and high implant energies without electronic stopping effects.

In the low-energy regime, the absence of electronic stopping effects was inconsequential, as shown in Figs. 1(a) and 2(a) since the stopping mechanism is dominated much by nuclear effects. With an increase in the initial kinetic energy of the incoming ion (Figs. 1(b) and 2(b)), exclusion of electronic stopping resulted in profiles with deep tails, showing poor agreement with the SIMS data. At high energies, the ion interacts mainly with the electrons in the target material; the energy transferred in the collision process is no longer negligible and the change in direction is significant. Because the stopping mechanism at high energies is dominated by electronic effects, the choice of the interatomic potential used was trivial, as shown by the indistinguishable profiles obtained with both ZBL and DMOL potentials. Conversely speaking, nuclear stopping is the dominant mode of energy transfer at low velocities where the ion can lose most of its energy in a single collision, changing its direction considerably. This is especially true for a heavy element like As (Fig. 2(a)) where the profiles obtained with different potentials differed significantly. While the disparity is less significant in the case of B (Fig. 1(a)), the use of the DMOL potentials yielded profiles which showed better agreement with experimental results in both cases. This can be largely attributed to the presence of an attractive well absent in the ZBL potential. Attractive forces while negligible at high ion velocities become non-trivial as the ion slows down and the ZBL potential fails to depict the right

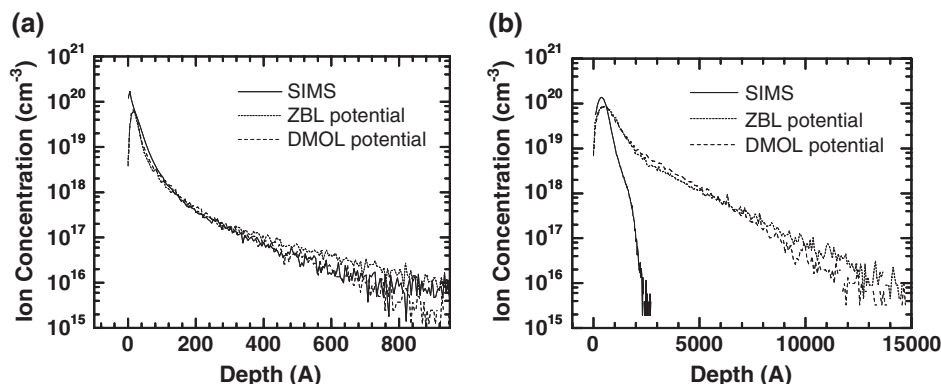


Fig. 1. Experimental and MD simulated (ZBL versus DMOL potential) profiles of B in Si (a) 0.5 keV, 5×10^{13} atoms/cm², 45°/0° (b) 10 keV, 1×10^{15} atoms/cm², 0°/0°.

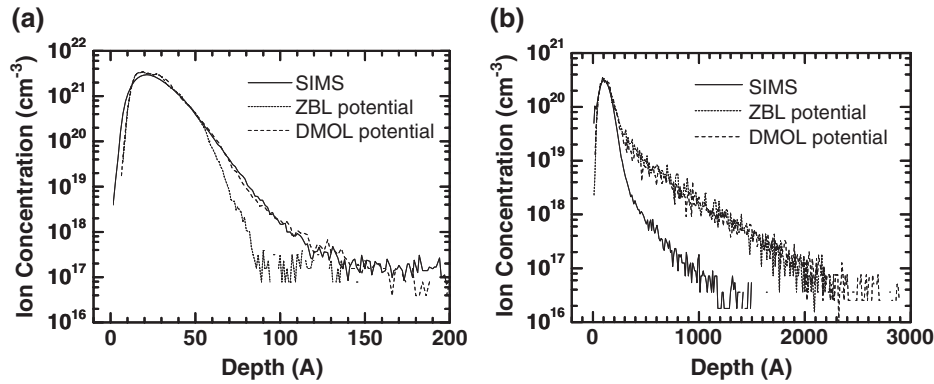


Fig. 2. Experimental and MD simulated (ZBL versus DMOL potential) profiles of As in Si (a) 1 keV, 1×10^{15} atoms/cm², $5.2^\circ/17^\circ$ (b) 10 keV, 5×10^{14} atoms/cm², $0^\circ/0^\circ$.

attractive nuclear forces at low energies. Henceforth, nuclear stopping is treated by the DMOL potentials. The accuracy of the potentials warrants the assumption that any discrepancies between the simulated and experimental results is caused by inaccuracies of the electronic stopping model.

2.2. Electronic effects: local versus non-local stopping

Separation of the energy loss of the ion into two separate components inherently assumes all possible correlations between the elastic nuclear collisions and inelastic losses due to electronic excitation to be negligible. This assumption is valid considering the correlation is insignificant when many collisions are averaged over, as when an ion penetrates a solid. Unlike atoms, quantum mechanics stipulates that electrons have strong wave characteristics and cannot be localised. Therefore electrons cannot be treated as point masses and an accurate description of electronic stopping is a much more complicated issue.

Electronic stopping parameterizations are either local or non-local. In local models, the scattering of the ion is dependent on the position in the crystal and largely on the electron charge density. In non-local models, the stopping is uniform throughout the crystal and independent of the density of the electrons. The charged ion is hindered by an induced drag force among the electron sea. The basis of many non-local electronic stopping models are based on the Brandt–Kitagawa (BK) theory [12] which factorizes the electronic stopping of a heavy ion into an effective charge and the electronic stopping of a proton. It does not take the shell structure of the ions' electron cloud into account, utilizing instead a centrosymmetric charge density which does not directly take into account the quantum mechanical stopping cross-section between the ion and the target atom electrons. One of the most popular non-local electronic stopping models based on the BK theory is formulated by Ziegler, Biersack and Littmark [1], the so-called ZBL stopping. In the ZBL model, the Fermi velocity is constant depending on the target material and can have an empirical correlation factor. The stopping of protons is obtained from a fit of 8 parameters that have different values in each elemental target material. In this work, the non-local ZBL model will be used in comparison to the local model described in the next section.

The local electronic stopping used in this work is based on the density-functional formalism and will be denoted as PENR (Puska, Echenique, Nieminen and Ritchie [13,14]) stopping henceforth. Unlike models based on the BK theory, the PENR model takes the structure of the ion's electron cloud into account and does not require any scaling factors. The local electronic stopping power S_E , of an ion traveling at velocity v ($v \leq$ Fermi velocity v_F) in a homogeneous electron gas can be expressed as in Eq. (1), where k_F is the Fermi momentum of electrons of the target, r_S is the one-electron radius (function of the electron density) and $\delta_l(E_F)$ is the phase shift at quantum number l for the scattering of an electron at the Fermi energy E_F .

$$S_E = \frac{3v}{k_F r_S^3} \sum_{l=0}^{\infty} (l+1) \sin^2[\delta_l(E_F) - \delta_{l+1}(E_F)] \quad (1)$$

This model is based on scattering phase shifts for Fermi-surface electrons [15]. The scattering phase shifts $\delta_l(E_F)$ can be determined within the density functional theory for atoms embedded in a homogeneous electron gas and are calculated in this work for $Z=5$ through $Z=51$ for a wide range of industrially important dopants. A dense grid of one-electron radius r_S values $0.1 \text{ \AA} \leq r_S \leq 6 \text{ \AA}$ is employed and components up to $l=10$ were used, although phase shifts for $l>5$ are very small. In cases where a self-consistent solution could not be obtained, which occurs for large Z (e.g. Indium: $Z=49$ and Antimony: $Z=51$), the Fermi phase shifts are calculated for a reduced grid of r_S values, and the tabulated values are then used in interpolating the phase shifts for a desired electron density. The anisotropy of the electron distribution is taken into account by using a three-dimensional charge distribution of silicon [16] calculated using the Dawson–Stewart–Coppens formalism [17–20] and the Hartree–Fock wave functions calculated by Clementi and Roetti [21].

The range profiles of light and heavy elements were simulated with both ZBL and PENR stopping models and compared against experimental SIMS data. Figs. 3 and 4 show the comparisons between both models for N and Sb, respectively. The poor agreement in the tail region of the sub-kiloelectronvolt N profile in Fig. 3(a) can be attributed to the high detection limit of N. Measurement of low level N concentrations requires good precision of SIMS instruments (improved vacuum and better primary beam intensity) and improved analysis protocol. Results shown represent the best

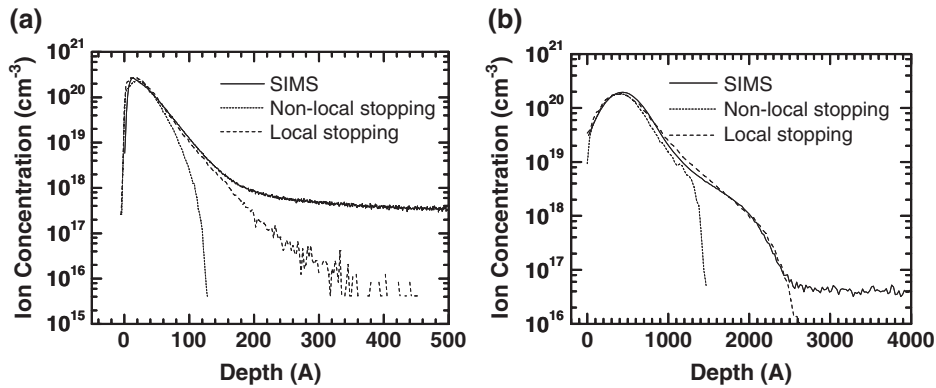


Fig. 3. Experimental and MD simulated (Non-local versus local electronic stopping) profiles of N in Si (a) 0.5 keV, $1e14$ atoms/cm², $0^\circ/0^\circ$ (b) 15 keV, $1e15$ atoms/cm², $5.2^\circ/17^\circ$.

detection limit under experimental constraints. The DMOL potentials have been employed for all simulations shown in this section; with all other simulation parameters kept constant, any discrepancies between the simulations can be solely attributed to the electronic stopping model. In all the cases shown, the local electronic stopping model produced profiles which show significantly better agreement with SIMS compared to the non-local ZBL model. The non-local model which assumes the stopping to be uniform throughout the crystal tends to underestimate the degree of channeling even in cases where channeling is not predominant, as in Figs. 3(b) and 4(b) where the implants are tilted 5.2° and 30° , respectively from the surface normal to reduce channeling effects. In cases where channeling is prevalent, especially in normal (Fig. 3(a)) and 45° tilted implants (Fig. 4(a)), the ZBL model overestimates the drag force due to the electrons, and produced profiles with much shallower junction depths than predicted by the local model and experiments.

The channeling of ions during the slowing down process has an important impact on the concentration profiles both in the vertical and lateral directions. In crystal channels, where the atomic and electronic densities are significantly lower than average, the importance of nuclear stopping is reduced relative to the electronic stopping and it is imperative that the electronic stopping model predict the ranges of the channeled ions accurately. From the results shown, it is obvious that the local

model is superior, especially where the electron density in a channel is significantly lower than in other directions. Contrary to the results of Sillanpaa et. al [16] which showed deficiencies of the PENR model in channeling directions, results in this work suggest that the PENR model remains accurate with 45° tilt angle. A wafer orientation of 45° in the azimuthal direction, in addition to the 45° tilt angle, represents one of the worst scenarios in axial and planar channeling [22] and Fig. 4(a) shows that the PENR model is still sufficiently accurate under such conditions for a slow heavy ion, without the need of a charge averaging scheme for improvement in the channels [16]. The model contains no free parameters and useful for any ion-target system where the electron distribution is known.

3. Conclusion

In this work, atomistic molecular dynamics simulations with nuclear effects treated with potentials calculated from density functional theory and electronic effects accounted for by a local electron stopping model based on Fermi phase shifts were used to predict range profiles for many industrially important dopants over a wide range of implant conditions. Profiles obtained with the commonly used repulsive universal ZBL potential, while adequate at high implant energies due to the dominance of electronic stopping over nuclear stopping, fails to describe the attractive forces that come into play at low ion

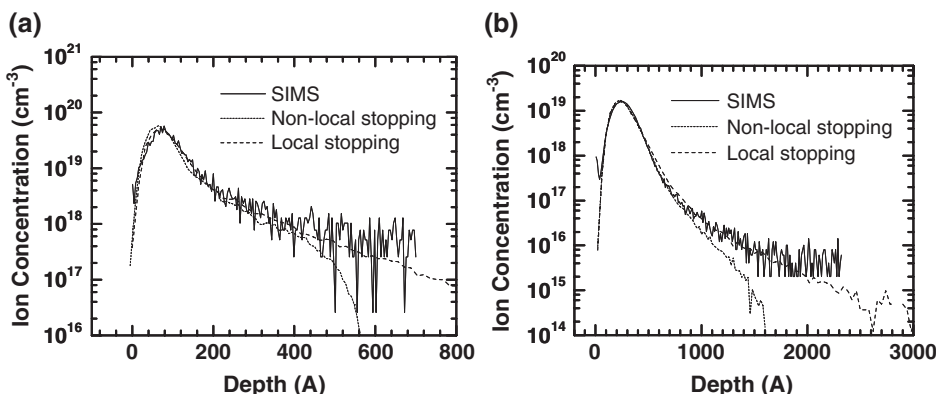


Fig. 4. Experimental and MD simulated (Non-local versus local electronic stopping) profiles of Sb in Si (a) 10 keV, $5e13$ atoms/cm², $45^\circ/45^\circ$ (b) 50 keV, $3.85e13$ atoms/cm², $30^\circ/0^\circ$.

velocities. Electronic stopping, on the other hand, proves to be crucial at both low and high ion velocities, especially when channelling effects are non-negligible. Non-local models like the ZBL model overestimate the stopping force due to electrons and give rise to ultra-shallow profiles. This is detrimental to transistor modelling which requires accurate ion implantation profiles for predicting device characteristics. Local models like the one used in this work, are able to predict accurately the final dopant positions and can be applied to any ion in any target whose electron distribution can be calculated without a parameter fitting process. The use of the universal potential and non-local electronic models should be exercised with caution since they provide inaccurate descriptions of the range profiles for certain non-calibrated species and underestimates the degree of channeling in the low and intermediate energy regime. On the contrary, local electronic models like the PENR model are capable of describing not only typical non-channeling implants, but its accuracy extends to describing long-ranged profiles propagated in crystal channels. Molecular dynamics coupled with accurate pair-specific DFT potentials and a phase-shift based electronic stopping model makes it a robust technique to predict dopant profiles in any implant direction at any energy for any species in question.

Acknowledgement

The authors would like to thank Prof. M. J. Puska and Dr J. Peltola for the electronic stopping code and all invaluable advice. All resources from National University of Singapore (NUS), Institute of High Performance Computing (IHPC) and

Agency of Science, Technology and Research (A*STAR) of Singapore are gratefully acknowledged.

References

- [1] J.F. Ziegler, J.P. Biersack, U. Littmark, *The Stopping and Range of Ions in Solids*, Pergamon Press, New York, 1985.
- [2] M. Hautala, *Phys. Rev.*, B 30 (1984) 5010.
- [3] M.T. Robinson, I.M. Torrens, *Phys. Rev.*, B 9 (1974) 5008.
- [4] S. Tian, *J. Appl. Phys.* 93 (2003) 5893.
- [5] K. Nordlund, *Comput. Mater. Sci.* 3 (1995) 448.
- [6] J. Sillanpaa, K. Nordlund, J. Keinonen, *Phys. Rev.*, B 62 (2000) 3109.
- [7] K.M. Beardmore, N. Gronbech-Jensen, *Phys. Rev., E Stat. Phys. Plasmas Fluids Relat. Interdiscip. Topics* 57 (1998) 7278.
- [8] J. Sillanpaa, K. Nordlund, J. Keinonen, *Phys. Scr.* T79 (1999) 272.
- [9] J. Peltola, K. Nordlund, J. Keinonen, *Nucl. Instrum. Methods Phys. Res., B Beam Interact. Mater. Atoms* 195 (2002) 269.
- [10] K. Nordlund, N. Runeberg, *Nucl. Instrum. Methods Phys. Res., B Beam Interact. Mater. Atoms* 132 (1997) 45.
- [11] DMOL is a trademark of Accelrys Inc. San Diego, California, USA.
- [12] W. Brandt, M. Kitagawa, *Phys. Rev.*, B 25 (1982) 5631.
- [13] P.M. Echenique, R.M. Nieminen, R.H. Ritchie, *Solid State Commun.* 37 (1981) 779.
- [14] M.J. Puska, R.M. Nieminen, *Phys. Rev.*, B 27 (1983) 6121.
- [15] T.L. Ferrell, R.H. Ritchie, *Phys. Rev.*, B 16 (1977) 115.
- [16] J. Sillanpaa, K. Nordlund, J. Keinonen, *Phys. Rev.*, B 62 (2000) 3109.
- [17] M. Deutsch, *Phys. Rev.*, B 45 (1992) 646.
- [18] B. Dawson, *Proc. R. Soc. Lond.*, A 298 (1967) 379.
- [19] R.F. Stewart, *J. Chem. Phys.* 58 (1973) 1668.
- [20] N.K. Hansen, P. Coppens, *Acta Crystallogr.*, A 34 (1978) 909.
- [21] E. Clementi, C. Roetti, *At. Data Nucl. Data Tables* 14 (1974) 177.
- [22] J.F. Ziegler, *Handbook of Ion Implantation Technology*, Elsevier Press, Amsterdam, 1992.